Available online at www.sciencedirect.com
SCIENCE DIRECT®
Materials Research Bulletin 40 (2005) 1136–1142
Materials Research Bulletin
www.elsevier.com/locate/matresbu

Aerosol-assisted vapor phase synthesis of powder composites in the target system GaN/TiN for potential electronic applications

Mariusz Drygaś [a], Cezary Czosnek [a], Robert T. Paine [b], Jerzy F. Janik [a,*]

[a] *AGH University of Science and Technology, Faculty of Fuels and Energy, Al. Mickiewicza 30, 30-059 Kraków, Poland*
[b] *University of New Mexico, Department of Chemistry, Albuquerque, NM 87131, USA*

Received 6 December 2004; received in revised form 17 March 2005; accepted 29 March 2005

Abstract

Synthesis and investigations of composites in the system GaN/TiN may help in understanding complex phenomena observed at GaN/titanium metal interfaces as well as expand a potential area of modern electronic/ceramic applications for such materials. Herein, powder composites in the system GaN/TiN are synthesized by means of the aerosol-assisted vapor phase synthesis (AAVS) method that was already successfully used to make nanopowders of BN and GaN as well as the magnetic semiconductor ''GaMnN''.

Keywords: A. Nitrides; A. Oxides; A. Ceramics; A. Electronic materials; B. Chemical synthesis

1. Introduction

In recent years, there has been a focused research interest in development of new synthetic routes to many nanocrystalline/nanopowder materials, mainly, due to predicted unique size-dependent materials properties in the nanosize region. In particular, the area of Group III(13) nitrides has become a fertile ground for numerous precursor chemistry endeavors as promises for utilization of such materials in electronics and ceramics seem to offer outstanding merits [1,2]. Gallium nitride, GaN, has notably been singled out among the nitrides, mostly, due to its potential in optoelectronics [3]. GaN is a broadband semiconductor designed for use in efficient light emitting or detecting devices in the now-accessible blue/violet range [4]. If one adds to this its relatively high thermal and chemical resistance, the advantage of

* Corresponding author. Tel.: +48 12 617 2577; fax: +48 12 617 2066.
E-mail address: janikj@uci.agh.edu.pl (J.F. Janik).

0025-5408/$ – see front matter © 2005 Elsevier Ltd. All rights reserved.
doi:10.1016/j.materresbull.2005.03.016

GaN over the classical semiconductors Si or Ge in manufacturing of high power transistors and switches is also of fundamental significance.

One of the challenges in new material development is tailoring the material's thermal and mechanical resistance by introducing new forms and/or improving the properties through suitable composite compositions. In this regard, titanium nitride TiN appears to be a good candidate to consider for improved GaN-based composites. For example, TiN is characterized by an outstanding hardness nearing that of diamond, very high melting point ~3000 °C, chemical resistance, and advantageous adherence properties towards a wide range of materials such as metals, semiconductors, and insulators [5]. Consequently, TiN is already used as friction protective coatings on many cutting tools. High electrical conductivity exceeding that of titanium metal and low temperature superconductivity are additional examples of the nitride's global properties [6]. Thin film optical characteristics of TiN (e.g., wavelength specific selective absorption of light) make this compound suitable for use in glass screens with adjustable light transmittance. TiN is used in microelectronics in the manufacture of VLSI devices serving as resistant and highly conductive diffusion barriers. The nitride's utilization in manufacturing of Shottky's diodes and MOS transistor gates has also been proposed [7].

It is worth mentioning that calculations have provided guidance for the incorporation of titanium ions into the crystal lattice of GaN and stabilization of solid solutions/doped lattices especially with cubic GaN [8]. In layered assemblages with hexagonal GaN, titanium nitride has been found to form and coexist in several simple and complex forms at Ti/GaN contacts of prototype electronic structures [9,10]. There have also been reports on advantageous properties of vapor-deposited thin films of TiN on GaN-layer templates for subsequent preparation of thick GaN wafers by metal hydride vapor phase epitaxy [11].

Considering the above, synergistic effects in the composite system of bulk powders of GaN/TiN could lead to enhanced mechanical, thermal, and structural properties relative to the pure nitrides and, therefore, to advantageous materials modifications. In this regard, the application of a synthetic approach to make the composites that relies on molecularly mixed gallium and titanium precursors followed by suitable nitridation of the mixture offers distinct advantages over physically/mechanically mixed nitrides. The resulting phase-heterogeneous mixture of the nitrides should have much better grain homogeneity as long as inter-granular growth, diffusion, and phase separation are controlled. It is also expected that investigations of the powder formation in the composite system GaN/TiN may provide a better understanding of the complex phenomena occurring at GaN/Ti–metal interfaces and yield composite materials, that upon compaction, yield useful materials forms for applications in modern electronics. Recent preliminary studies, conducted in collaboration with the Institute of High Pressure Physics, Polish Academy of Sciences, Warsaw, Poland, on PT sintering of nanocrystalline pure GaN and GaN-based composite powders suggest the possibility of manufacturing mechanically robust GaN/GaN-based pellets in this way. Based on that, we plan in the near future to prepare such GaN/TiN sintered compacts and use them as alternative to GaN single crystal inexpensive nitride supports for growing selected microelectronic structures as well as thick GaN wafers.

2. Experimental

Syntheses of GaN and TiN and composite powders were accomplished by application of the published aerosol-assisted synthesis that was previously used to prepare powders of pure BN [12] and GaN [13] as well as the magnetic semiconductor "GaMnN" [14].

2.1. Aqueous solutions

Commercial $Ga(NO_3)_3 \cdot xH_2O$ (Aldrich, $x = 2$) was used as the gallium precursor while in situ prepared $Ti(NO_3)_4$ and $TiCl_4$ solutions were used as titanium sources. Aqueous $TiCl_4$ solutions were prepared as follows. Liquid titanium chloride (0.05 mol; 9.5 g or 5.5 mL) was slowly added dropwise (1 h) to 495 mL of deionized water at 0 °C affording a 0.1 M solution of Ti^{+4}. Aqueous solutions of $Ti(NO_3)_4$ were prepared according to the published procedure [15]. The fresh solutions containing Ti^{+4} were individually mixed with a suitable amount of 0.12 M solution of Ga^{+3} to yield solutions with atomic ratio $Ga^{+3}/Ti^{+4} = 5/1$. An aerosol mist of the solution was generated by using an ultrasound transducer and the aerosol was passed in a stream of N_2 carrier gas at 1 L/min to a horizontal ceramic tube reactor maintained at 1000 °C. An accompanying flow of nitriding NH_3 was introduced to the reactor at 3 L/min. The solution was usually aerosolized at a rate of ~30 mL/h for 10 h. Typically, 1.0–1.5 g of raw greenish powder was collected on a nylon filter placed at the reactor exit. The raw powders were additionally pyrolyzed at 1000 °C for 6 h under a NH_3 flow of 1 L/min to complete the nitridation. The final products were recovered as dark brown to black powders.

2.2. Methanol solutions

For aerosol formation, freshly made methanol solutions of titanium tetramethoxide $Ti(OCH_3)_4$ stabilized with HNO_3 (1.5 mL of concentrated NHO_3 per 1 L of CH_3OH) were combined with suitable proportions of $Ga(NO_3)_3 \cdot xH_2O$ ($x = 2$) to yield atomic ratio Ga/Ti = 5/1. Freshly prepared solutions were transparent; however, their colloidal nature was evidenced by the Tyndall effect. In typical syntheses, the rate of aerosol generation was ~80–90 mL/h and the generation time, 10 h. Brown-tinted powders were recovered from the aerosol reactor after this stage and they were subjected to additional nitriding pyrolyses at 1000 °C for 6 h under a NH_3 flow of 1 L/min.

All powders were characterized by XRD and SEM/EDX. Additionally, helium densities and residual oxygen contents were determined.

3. Results and discussion

In general, the aerosol method is well suited to make complex composite systems mixed on a molecular level. In the current case, the fixed initial atomic ratio of gallium and titanium ions was achieved both in fresh aqueous and methanol solutions. However, slow colloid formation appeared gradually over the course of days. The presence of small concentrations of HNO_3 retards the colloid formation while increased aerosol generation temperatures are detrimental for stabilization of the clear solutions. In this regard, the colloidal nature of the precursor solution mixtures should, in principle, constitute a good template for the evolution of nanosized solid particles via aerosol droplet generation provided the colloid is sufficiently stable under the aerosol process conditions.

In the initial stage of the aerosol generation, aerosol droplets consisting of a precursor solution are transported in a stream of the N_2 carrier gas and nitriding NH_3 through the heated reactor tube held at 1000 °C. Numerous physical and chemical changes take place during the droplet passage including the evaporation of solvent, thermally driven decomposition of the precursors to oxides, and surface and interior nitridation. Mainly due to relatively short residence times in the hot reaction zone (10–60 s), the

nitridation reactions in this stage proceed only partially to completion. This has been confirmed by elemental analysis (oxygen contents) and spectroscopic methods. In the case of the methanol solutions, carbothermal reduction reactions play a role leading to lower residual oxygen contents in the raw powders compared to aqueous solution cases. Similar results are well documented for the aerosol synthesis of BN [16]. In the second stage of the powder synthesis, bulk powder pyrolysis under an ammonia atmosphere was carried out. The pyrolysis conditions (1000 °C, 6 h, flow of NH_3) were suitably adjusted to maximize nitridation, especially, for the titanium component, while minimizing detrimental side-reactions such as sublimation of GaN out of the composite system accompanied by concomitant decomposition to metallic Ga.

All final powder products showed similar dark brown to black coloration. The XRD study confirmed that the dominant crystalline phase in most cases was hexagonal GaN, h-GaN (Fig. 1). Another major phase was tentatively identified as cubic TiN, c-TiN (vide infra). The powders derived from the systems $Ga(NO_3)_3{\cdot}xH_2O/Ti(NO_3)_4$ and $Ga(NO_3)_3{\cdot}xH_2O/Ti(OCH_3)_4$ also contained small quantities of the cubic phase c-GaN that was refined from peak deconvolution of the diffraction patterns (e.g., see the characteristic peak for c-GaN visible at $2\theta = 40.16^\circ$) [17]. It is worth noting that the relative proportion of c-GaN in these composites usually increased with pyrolysis times up to 10 h in the second stage.

Based on peak positions, the crystallographic cell dimensions were calculated for all present crystalline phases (Table 1).

The calculated cell parameters for h-GaN and c-GaN are very close to those reported for the pure phases. More significant differences are found in the *a*-parameters for c-TiN, 4.222–4.227 Å, and the reported value for the pure phase, 4.24 Å. This discrepancy can be linked to the specifics of nitridation of the titanium-bearing precursors where in the initial stages the formation of transient TiO species takes

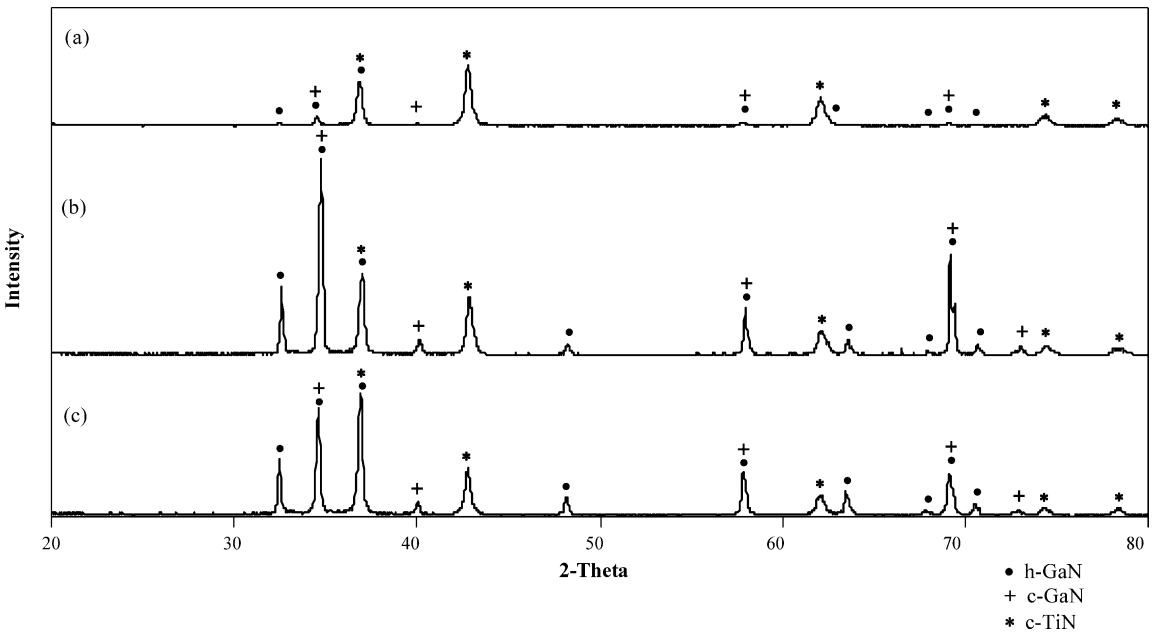

Fig. 1. XRD diffraction patterns for composites in the systems: (a) $Ga(NO_3)_3{\cdot}xH_2O/TiCl_4$ (aqueous), (b) $Ga(NO_3)_3{\cdot}xH_2O/Ti(NO_3)_4$ (aqueous) and (c) $Ga(NO_3)_3{\cdot}xH_2O/Ti(OCH_3)_4$ (methanol solution).

Table 1
Crystallographic cell parameters for crystalline phases and residual oxygen contents in the composites

Precursor system	h-GaN (Å)	c-GaN (Å)	c-TiN (Å)	O (wt.%)
$Ga(NO_3)_3{\cdot}xH_2O/TiCl_4$ (aqueous)	3.189, 5.178	–	4.224	3.71
$Ga(NO_3)_3{\cdot}xH_2O/Ti(NO_3)_4$ (aqueous)	3.188, 5.181	4.502	4.227	1.58
$Ga(NO_3)_3{\cdot}xH_2O/Ti(OCH_3)_4$ (methanol solution)	3.187, 5.181	4.502	4.222	1.69

place. In this regard, TiO despite its nominal +2 oxidation state is a known nonstoichiometric compound of Ti^{+4} characteristic of heavily defected lattices with systematic and random absences of cubic symmetry [18]. This phase under the reaction conditions would undergo gradual nitridation via an oxygen displacement mechanism to yield transient oxynitrides TiO_xN_y and, eventually, conditions permitting, resulting in complete nitridation to yield the target product TiN. The oxynitrides can be thought of as solid solutions of the related cubic phases of TiN (a = 4.24 Å) and TiO (a = 4.17 Å) with the a-parameter ranging between the two limits according to the Vegard's law. Other things being equal, the a-parameter for the cubic titanium-bearing phase can bring about a useful estimation of the nitridation progress. The use of the notation of c-TiN in Table 1 is therefore a somewhat simplified label for the titanium nitride that still may contain some structural oxygen. A separate study on nitridation of AAVS produced titanium-only precursor powders that give pure TiN will be published elsewhere [19].

Residual oxygen content in the composites was also examined. The highest O-content, 3.71 wt.%, was found in the composite from the system $Ga(NO_3)_3{\cdot}xH_2O/TiCl_4$ (aqueous). In the remaining two composites the oxygen contents were approximately twice as low (Table 1). This is consistent with the former product being the most severely depleted in gallium. This in turn suggests that the residual oxygen is mostly associated with titanium, i.e., in oxynitrides TiO_xN_y and it is consistent with the previous discussion of the crystallographic cell data for the transition from c-TiO through solid solutions c-TiO_xN_y to c-TiN.

The helium density data are in qualitative agreement with the above. Namely, the measured composite densities lie between the theoretical values for pure TiN and GaN (Table 2). The determined density values also support the experimental fact of gallium depletion (and enrichment in the Ti-component) from these systems during the 1000 °C pyrolysis. The composite obtained from the methanol solution-based system is characterized by a relatively highest density, which implies here the smallest gallium losses among the products. Another possible interpretation of this fact that is related to the formation of TiO/GaN rather than TiN/GaN (similar intermediate densities expected) is not consistent with the low oxygen content in the composite.

Table 2
Helium densities of composites and reference compounds

Precursor system	d_{He} (g/cm^3)	S.D. (g/cm^3)
$Ga(NO_3)_3{\cdot}xH_2O/TiCl_4$ (aqueous)	5.6204	0.0411
$Ga(NO_3)_3{\cdot}xH_2O/Ti(NO_3)_4$ (aqueous)	5.6873	0.0087
$Ga(NO_3)_3{\cdot}xH_2O/Ti(OCH_3)_4$ (methanol solution)	5.9483	0.0296
GaN (reference material)	$6.0886_{theor.}$	–
TiN (reference material)	$5.4240_{theor.}$	–
TiO (reference material)	$5.807_{theor.}$	–

Table 3
Average crystallite sizes calculated with Scherrer's equation

Precursor system	h-GaN (nm)	c-GaN (nm)	c-TiN (nm)
$Ga(NO_3)_3{\cdot}xH_2O/TiCl_4$ (aqueous)	35	–	23
$Ga(NO_3)_3{\cdot}xH_2O/Ti(NO_3)_4$ (aqueous)	40	34	23
$Ga(NO_3)_3{\cdot}xH_2O/Ti(OCH_3)_4$ (methanol solution)	35	34	24

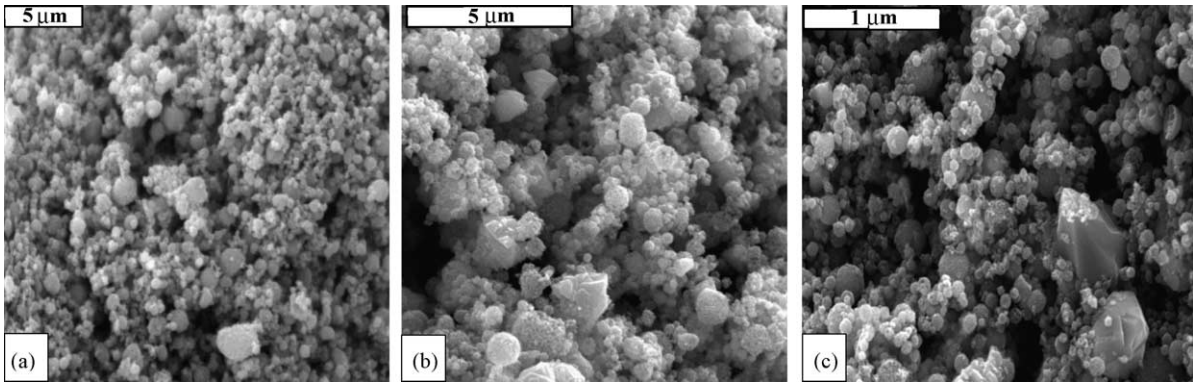

Fig. 2. SEM images for composite powders prepared from the systems: (a) $Ga(NO_3)_3{\cdot}xH_2O/TiCl_4$ (aqueous), (b) $Ga(NO_3)_3{\cdot}xH_2O/Ti(NO_3)_4$ (aqueous), and (c) $Ga(NO_3)_3{\cdot}xH_2O/Ti(OCH_3)_4$ (methanol solution).

Average crystallite sizes for the three detected phases in the composites were calculated, where possible, from the Scherrer's equation applied to high intensity low angle diffractions in the XRD patterns (Table 3). The sizes determined for h-GaN, 35–40 nm range, were typical for the method and applied conditions. Rather unexpected was the appearance of the cubic phase of GaN, c-GaN, with crystallites in the nanosize range, 34 nm. The c-TiN component of the composites was characterized with the relatively smallest crystallites of 23–24 nm.

The powder composites displayed somewhat similar scanning electron micrograph morphologies although some variations were found between the different solvent systems (Fig. 2). The smaller size particles have a generally spheroidal shape although these particles tend to be agglomerated. Large and blocky crystallites also appear in the systems $Ga(NO_3)_3{\cdot}xH_2O/Ti(NO_3)_4$ (aqueous) (Fig. 2b) and $Ga(NO_3)_3{\cdot}xH_2O/Ti(OCH_3)_4$ (methanol solution) (Fig. 2c). In the system $Ga(NO_3)_3{\cdot}xH_2O/TiCl_4$ (aqueous), the smaller spheroidal particles appear to be extensively deformed and visibly agglomerated (Fig. 2a). The EDX analysis suggests that the blocky crystallites contain gallium nitride while the smaller spheroidal features consist of titanium nitride.

4. Conclusions

The aerosol-assisted synthesis of powder composites GaN/TiN employing both aqueous and methanol solutions of commercially available and affordable precursors is efficient. Based on the XRD and EDX data, the composites are shown to contain mostly hexagonal GaN and cubic TiN admixed with a minor phase of cubic GaN. This is also consistent with helium density data. Detailed analysis of the

crystallographic cell parameters and residual oxygen contents of the composites suggests that the nitridation process of the oxygen-bearing titanium precursors is process limited and occurring in a gradual way. Namely, after preliminary precursor decomposition under reducing reaction conditions to cubic TiO (mostly, aerosol generation stage), oxygen displacement by nitrogen takes place via formation of the intermediate cubic oxynitride TiO_xN_y eventually yielding the target cubic TiN still containing some structural oxygen (pyrolysis stage). Similar changes for the gallium precursor are mostly completed under applied conditions. The SEM images show for all composites similar bimodal morphologies with smaller spheroidal features made of TiN and larger blocky crystallites made of GaN. From XRD diffraction patterns, the average crystallite sizes for h-GaN are in the range 35–40 nm, for c-GaN centered at about 34 nm and for c-TiN somewhat smaller at about 24 nm. Other analytical data indicate that the product powders are depleted in gallium versus the initial ratio Ga/Ti = 5/1, most likely due to sublimation and decomposition of the GaN component under the pyrolysis conditions utilized. In continuing studies, the powder composites will be pressed/sintered into mechanically stable thin compacts to afford a novel nitride materials form with great potentials for utilization in microelectronics.

Acknowledgements

JFJ wants to acknowledge the generous support of Polish Committee for Scientific Research KBN Grant No. 3 T08D 043 26. RTP acknowledges funding from the U.S. National Science Foundation (CHE-9983205) that has supported this international cooperation.

References

[1] V.G. Golubev, D.A. Kurdyukov, A.V. Medvedev, A.B. Pevtsov, L.M. Sorokin, J.L. Hutchison, Semiconductors 35 (2001) 1320.
[2] H. Morkoç, Mater. Sci. Eng. B43 (1997) 137.
[3] W. Han, A. Zettl, Appl. Phys. Lett. 80 (2002) 303.
[4] Y. Arakawa, IEEE J. Sel. Top. Quant. 8 (2002) 823.
[5] L.H. Dubois, Polyhedron 13 (1994) 1329.
[6] R.M. Fix, R.G. Gordon, D.M. Hoffman, Chem. Mater. 2 (1990) 235.
[7] R.M. Fix, R.G. Gordon, D.M. Hoffman, Chem. Mater. 3 (1991) 1138 (and references therein).
[8] J.A. Chisholm, P.D. Bristowe, Comput. Mater. Sci. 22 (2001) 73.
[9] C.J. Lu, A.V. Davydov, D. Josell, L.A. Bendersky, J. Appl. Phys. 94 (1) (2003) 245.
[10] S. Gautier, Ph. Komninou, P. Patsalas, Th. Kehagias, S. Logethitidis, C.A. Dimitriadis, G. Nouet, Semicond. Sci. Technol. 18 (2003) 594.
[11] A. Usui, T. Tchihashi, K. Kobayashi, H. Sunakawa, Y. Oshima, T. Eri, M. Shibata, phys. stat. sol. (A) 194 (2) (2002) 572 (and references therein).
[12] E.A. Pruss, G.L. Wood, W.J. Kroenke, R.T. Paine, Chem. Mater. 12 (2000) 19.
[13] G.L. Wood, E.A. Pruss, R.T. Paine, Chem. Mater. 13 (2001) 12.
[14] J.F. Janik, M. Drygaś, C. Czosnek, M. Kamińska, M. Palczewska, R.T. Paine, J. Phys. Chem. Sol. 65 (2004) 639.
[15] C.H. Jung, D.K. Kim, J. Mater. Synth. Process. 10 (2002) 23.
[16] R.T. Paine, W.J. Kroenke, E.A. Pruss, G.L. Wood, J.F. Janik, Organoboron route and process for preparation of boron nitride, US Patent No. 6,824,753 B2, 30 November 2004.
[17] R.J. Jouet, A.P. Purdy, R.L. Wells, J.F. Janik, J. Clust. Sci. 13 (4) (2002) 469 (and references therein).
[18] D. Watanabe, J.R. Castles, Acta Cryst. 23 (1967) 307.
[19] M. Drygaś, R.T. Paine, J.F. Janik, in preparation.